Supplementary information for:

Photoluminescence modal splitting via strong coupling in hybrid Au/WS_2/GaP nanoparticle-on-mirror cavities

Merve Gülmüs,[a] Thomas Possmayer,[a] Benjamin Tilmann,[a] Paul Butler,[b,c] Ian D. Sharp,[b,c] Leonardo de S. Menezes,[a,d] Stefan A. Maier,[e,f] Luca Sortino[a†]

[a1]*Chair in Hybrid Nanosystems, Nanoinstitute Munich, Faculty of Physics, Ludwig-Maximilians-Universität München, 80539 Munich, Germany*

[b]*Walter Schottky Institute, Technische Universität München, Am Coulombwall 4, 85748 Garching, Germany*

[c]*Physics Department, TUM School of Natural Sciences, Technische Universität München, Am Coulombwall 4, 85748 Garching, Germany*

[d]*Departamento de Física, Universidade Federal de Pernambuco, 50670-901 Recife-PE, Brazil*

[e]*School of Physics and Astronomy, Monash University, Clayton, Victoria 3800, Australia*

[f]*The Blackett Laboratory, Department of Physics, Imperial College London, London, SW7 2BW, United Kingdom*

Supplementary Note 1: Methods

Sample fabrication Nanoantennas were fabricated using top-down lithographic methods. The process began with the coating of a SiO_2 substrate with a 100 nm layer of GaP grown at 350 °C and an additional 80 nm thick layer of SiO_2, using an Angstrom sputtering system with deposition rates of 0.20 Å s^{-1} and 0.23 Å s^{-1}, respectively. A double layer comprising an electron-sensitive resist of polymethylmethacrylate (PMMA) along with a conductive layer used to prevent charging effects during patterning were then spin-coated onto the sample. Nanoantennas were designed to maintain a 5 μm spacing to prevent interaction between adjacent nanoantennas and enable accurate single-particle measurements. Electron beam lithography patterning was then conducted using a Raith eLine system by applying a dosage of 330 μC cm^{-2} at an external high voltage of 30 kV via a 20 μm aperture. Development was performed by immersing the sample in a solution containing methyl-isobutyl-ketone (MIBK) and isopropanol in a 1:3 ratio. A 3 nm Ti layer, which served as an adhesive layer, and a 30 nm Au layer, which was used as an etch mask, were then deposited using an electron beam evaporator. In the lift-off process, the PMMA was removed from the sample by immersing it in Microposit Remover overnight. The etching process was carried out using a RIE system from Oxford Instruments. Initially, the SiO_2 layer was selectively etched using RIE, while the gold layer was etched using Gold Etchant Standard (KI/I_2). The remaining SiO_2 on the sample served as a mask for the subsequent GaP RIE step and was removed with an additional RIE etching step. WS_2 monolayers were obtained using the mechanical exfoliation method from bulk WS_2 crystals (HQ Graphene) onto polydimethylsiloxane (PDMS). WS_2 monolayers were transferred onto the target nanoantennas using an all-dry viscoelastic stamping method in a custom-built transfer setup.

Fabrication of metallic mirrors For the fabrication of the gold mirror, 3 nm Cr film and gold films of various thicknesses were deposited on a sapphire substrate by sputtering, at a rate of 15 Å s^{-1} and pressure of 2.2 x 10^{-2} mbar. From AFM measurements, we extract the RMS roughness as a function of the gold film thickness, found to be below 1 nm for gold film of 50 nm thickness (Figure S1a). Figure S1b shows the 1 μm x 1 μm AFM scan of an Au film of 50 nm thickness deposited via sputtering. The 3 nm Al_2O_3 dielectric spacer was deposited on the gold mirror via atomic layer deposition (ALD) in a Veeco Fiji G2 system, at a temperature of 200 °C.

Trimethylaluminum (TMA) was used as a reactant and H_2O as the co-reactant. Each cycle consists of a 0.08 s TMA pulse, 20 s Ar purge, 0.08 s H_2O pulse, and 20 s Ar purge. During the deposition, the chamber was kept at a base pressure of 0.1 Torr, and the carrier Ar flow was set to 120 sccm. The thickness of the resulting alumina film was monitored with in-situ spectroscopic ellipsometry measured on a silicon chip that was placed in the reactor together with the samples.

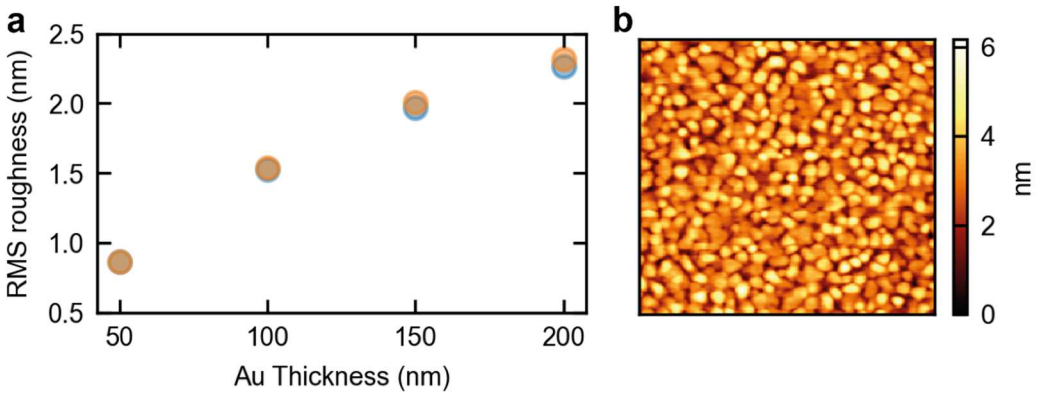

Figure S1: (a) RMS roughness extracted from 1 µm x 1 µm AFM images of gold films deposited via sputtering. Data shown for two different samples (blue and orange dots). (b) 1 µm x 1 µm AFM scan of a 50 nm thick gold film deposited via sputtering.

Numerical simulations Numerical simulations were performed according to the finite-difference time-domain (FDTD) method using commercial software (Ansys Lumerical). The refractive index of the amorphous GaP film was determined by in-house ellipsometry measurements.

Optical spectroscopy Darkfield scattering spectroscopy and room temperature PL measurements were conducted with a commercial spectrometer from WiTech (Alpha 300), which employs a broadband white light source and a continuous wave (CW) 532 nm green laser for excitation and a 100x objective (0.9 numerical aperture). The light was collected through the same objective and was directed to a monochromator and CCD system (Princeton Instruments) with a multimode optical fiber for detection.

Supplementary Note 2: PL spectroscopy for off-resonance GaP nanoantennas

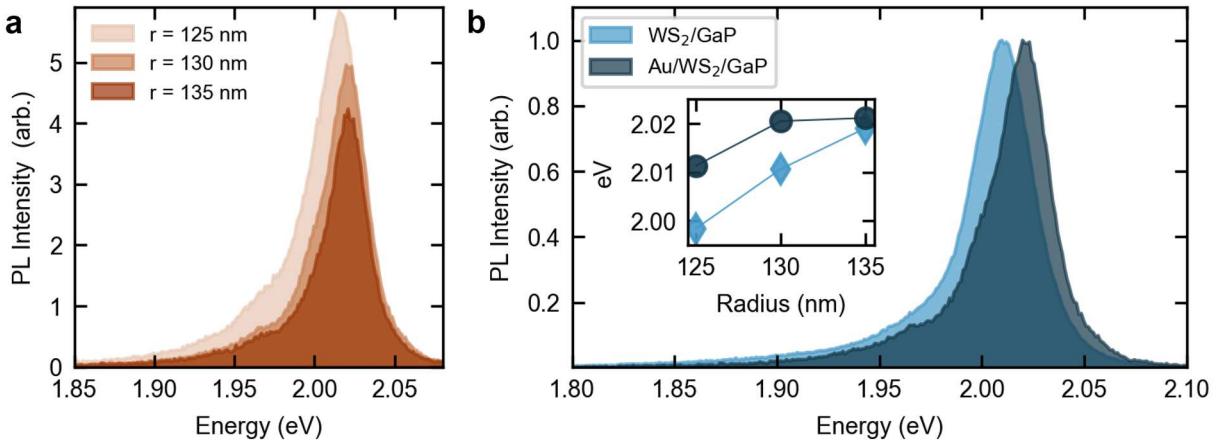

Figure S2. (a) WS_2 monolayer PL emission when coupled to off-resonance GaP nanoantennas. (b) Comparison of the WS_2 PL emission spectra coupled to GaP nanoantenna (radius 130 nm) with and without the gold mirror. Inset: exciton peak blueshift for off-resonance antennas with the gold mirror (circle markers), and without (diamond markers).

Supplementary Note 3: Numerical FDTD simulations

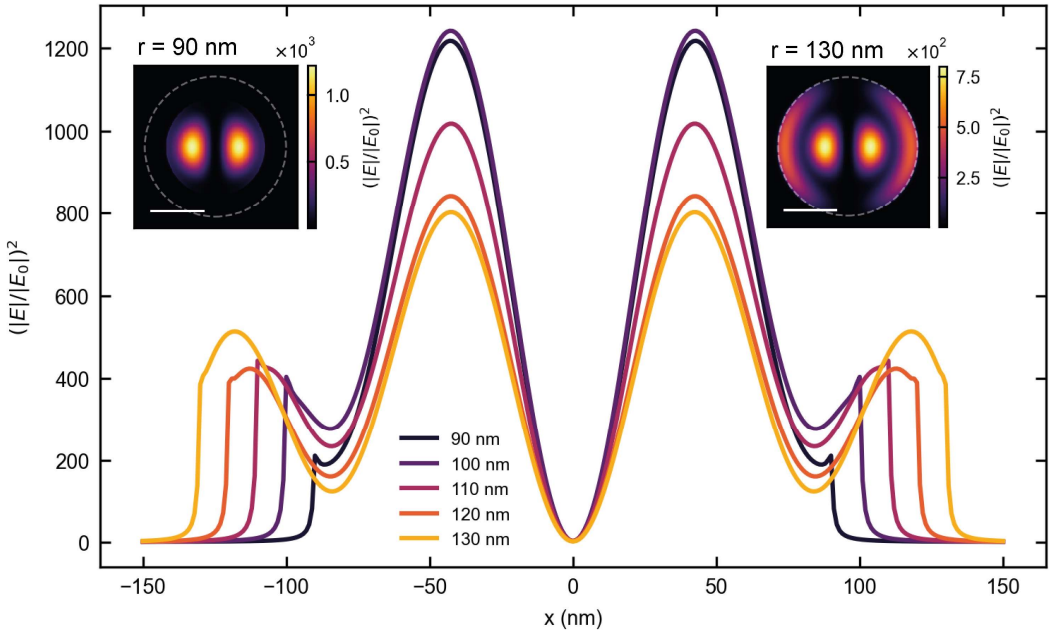

Figure S3. FDTD simulations of the electric field enhancement in the nanogap region, for GaP nanoantennas with different radii, and collected at 619 nm. The inset shows the electric field enhancement, $(|E|/|E_0|)^2$, in the x-y plane of a hybrid nanocavity, taken 0.5 nm above the mirror surface, with GaP nanoantenna with radius of 90 nm (left) and 130 nm (right). Scale bars: 100 nm

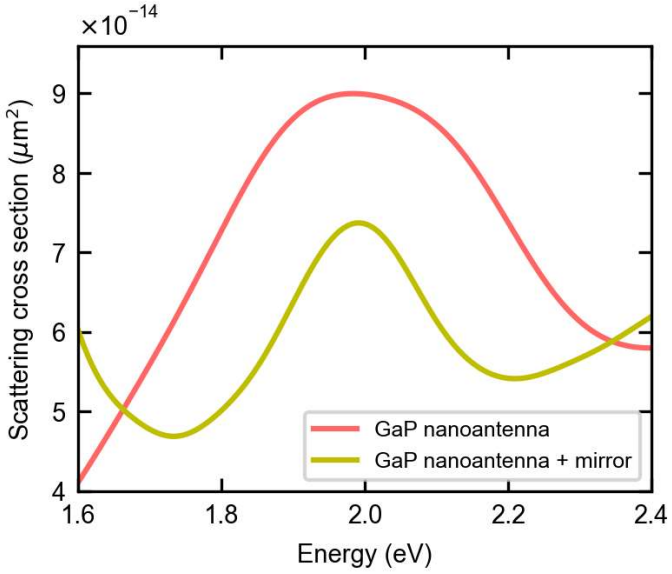

Figure S4. FDTD simulations of the scattering cross-section for a single GaP nanoantenna (in red), with radius of 90 nm and 100 nm height, and for the same nanoantenna on a gold mirror (in yellow) with 3 nm of Al_2O_3.

Supplementary Note 4: Dark field scattering of the hybrid particle-on-mirror cavity

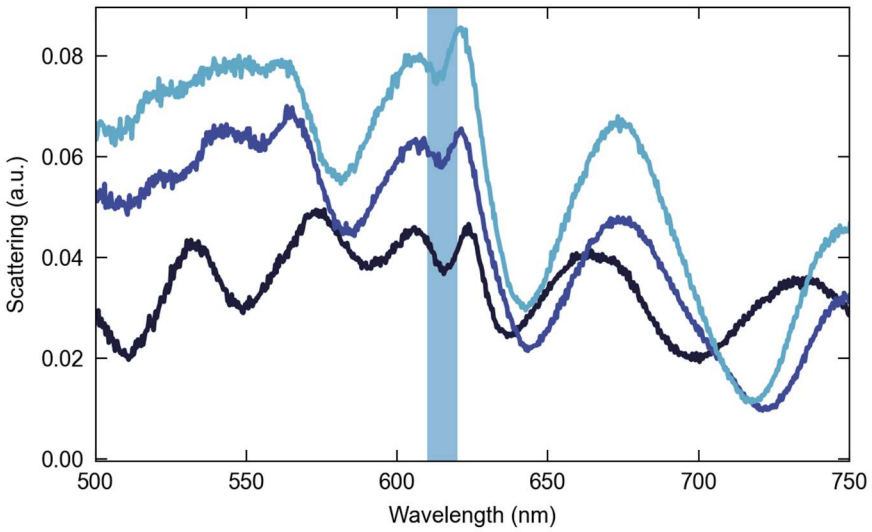

Figure S5. Dark field scattering of a hybrid nanocavity (GaP nanoantenna radius = 100 nm), for slightly different positions on the sample. The excitation is from the glass side, exhibiting strong interference fringes caused by the 150 µm thick glass slide. The blue shaded area corresponds to the WS_2 exciton resonance dip, with an energy splitting of approximately 50 meV.

Supplementary Note 5: Voigt profile fitting

The Voigt profile, $V(x,\sigma,\gamma)$, is a convolution of a Gaussian, $G(x',\sigma)$, and Lorentzian, $L(x',\gamma)$, profile:

$$V(x,\sigma,\gamma) = \int_{-\infty}^{\infty} G(x',\sigma)\ L(x-x',\gamma)dx'$$

where σ is the standard deviation of the Gaussian profile, and γ is the half-width at half-maximum (HWHM) of the Lorentzian profile. It can be implemented to extract the relative weight of the two parameters from the linewidth of radiative transitions. Figure S5 shows the Lorentzian (W_L, square markers) and Gaussian (W_G, round markers) weight of the Voigt profile, extracted from the data shown in Figure 4b in the main text. The lower polariton peak is characterized by a mixed Lorentzian and Gaussian character at low excitation powers, shifting to a predominant Lorentzian profile at high excitations. For the upper polariton branch, a similar trend is observed. On the contrary, the exciton peak is dominated by a Gaussian profile, independent of the excitation power, as expected from the strong inhomogeneous broadening of 2D excitons at room temperature. Moreover, the values of the Lorentzian weight, which can be associated with the homogeneous linewidth of the exciton emission, are close to the reported value > 10 meV [1].

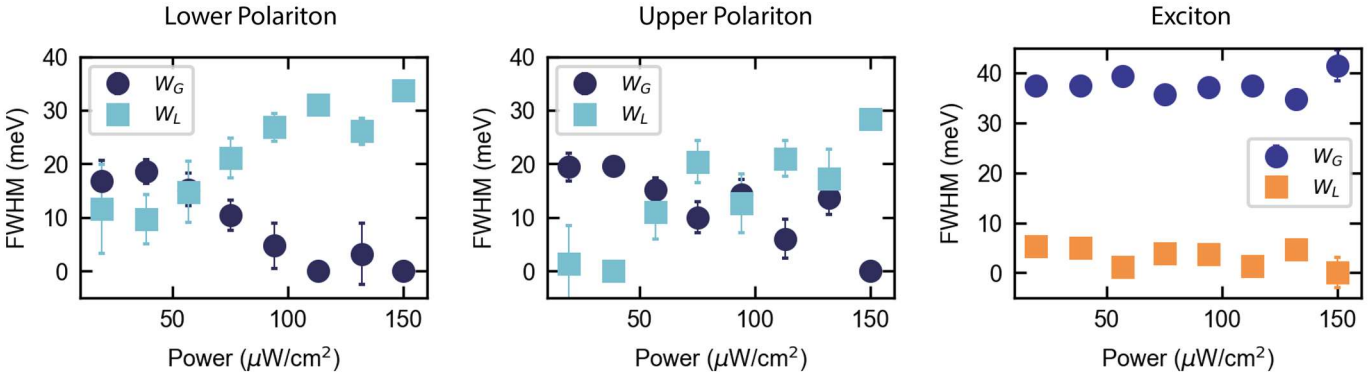

Figure S5. Relative Lorentzian, W_L, and Gaussian, W_G, weight of the Voigt profile, extracted from the PL spectra a WS_2 monolayer shown in Figure 4b in the main text.

Supplementary Note 6: Coupled oscillator model fit parameters

A	g (meV)	ω_{cav} (eV)	ω_X (eV)	κ (meV)	γ (meV)
0.202 ± 0.001	96.3 ± 2.2	1.983 ± 0.001	1.966 ± 0.01	380 ± 3.5	90 ± 4.6

Supplementary Table 1: Fit parameters for the data shown in Figure 2b, using Equation 3 in the main text.

A'	Ω_R (meV)	ω_{cav} (eV)	ω_X (eV)	κ (meV)	γ (meV)
0.126 ± 0.001	15.3 ± 0.01	1.973 ± 0.001	1.975 ± 0.01	50.0 ± 3.2	20.5 ± 4.1

Supplementary Table 2: Fit parameters for the data shown in Figure 3e, using Equation 4 in the main text.

References

(1) Cadiz, F.; Courtade, E.; Robert, C.; Wang, G.; Shen, Y.; Cai, H.; Taniguchi, T.; Watanabe, K.; Carrere, H.; Lagarde, D.; Manca, M.; Amand, T.; Renucci, P.; Tongay, S.; Marie, X.; Urbaszek, B. Excitonic Linewidth Approaching the Homogeneous Limit in MoS_2-Based van Der Waals Heterostructures. *Phys. Rev. X* **2017**, *7* (2), 1–12. https://doi.org/10.1103/PhysRevX.7.021026.